

The uses of non-steady-state membrane characterisation techniques for the study of transport properties of active layers of nanofiltration membranes: theory with experimental examples

Andriy E. Yaroshchuk^{a,b,*}, Volker Ribitsch^b

^a *Institute of Bio-Colloid Chemistry, National Academy of Sciences of Ukraine, Kiev, Ukraine*

^b *Institut für physikalische Chemie, Karl-Franzens-Universität, Heinrichstr. 28, 8010 Graz, Austria*

Abstract

Nanofiltration (NF) is a relatively new membrane process suitable for the separation of solutes of close molecular weight. The rejection mechanisms of nanofiltration membranes have not been reliably identified, yet. The electrostatic repulsion of coions by fixed membrane charge (Donnan exclusion) is considered one of most probable rejection mechanisms. However, practically no direct information on the electrochemical and/or electrokinetic properties of NF membranes is available. The interpretation of conventional electrochemical and/or electrokinetic measurements with NF membranes is complicated by their multilayer structure. Under linear conditions only average membrane transport properties can be obtained from steady-state measurements. Information on the properties of constituent layers can be obtained from non-steady-state and/or non-linear measurements, alone. In this paper the opportunities offered by non-steady-state techniques are explored. Volume flows and changes in solute concentration cannot usually be observed at sufficiently short times when the system is still far away from steady state. Therefore the only suitable response is electrical. It is not immediate due to the concentrational polarisation of boundaries between membrane constituent layers. The theory of transient membrane potential, transient filtration potential and low-frequency electrical impedance is briefly presented. The suitability of various non-steady state techniques for the determination of transport and accumulation properties of constituent layers of NF membranes is discussed and compared with available experimental data on transient membrane potential. It is concluded that each of techniques has its advantages and drawbacks. Therefore, the application of several techniques to the same system is desirable for the minimisation of systematic errors. © 2000 Published by Elsevier Science B.V.

Keywords: Nanofiltration; Non-steady-state; Electrical response; Active layer; Fixed charge density

1. Introduction

Nanofiltration (NF) is a relatively new membrane process suitable for the separation of solutes of close molecular weight. Knowing the rejection mechanisms of NF membranes is important for the selection of optimal membranes and operational conditions for a given application. However, the rejection mechanisms of nanofiltration membranes have not been reliably identified, yet. The electrostatic repulsion of coions by the fixed membrane charge (Donnan exclusion) is considered one of most probable rejection mechanisms. Quite a lot has recently been published on the modelling of NF within the scope of the so called fixed-charge-steric-hindrance model [1–9]. However, in all of those papers the fixed charge density is, in fact, considered an adjustable parameter to be determined from the fitting of a theoretical model to the experimental data on salt

rejection and membrane hydraulic permeability. Practically no independent information on the electrochemical and/or electrokinetic properties of NF membranes is available. Mainly streaming potentials along membrane surface have been measured [10,11]. They can be interpreted in terms of fixed charge density at the external membrane surface. That parameter may be important, e.g. for understanding the membrane fouling by charged colloids [12–15]. However, it evidently may have little in common with the fixed charge density at the internal pore surface. An attempt to measure the streaming potential across NF membranes have been done by Lemordant et al. [16,17]. However, the interpretation of their measurements in terms of active layer properties is impossible without independent (and hardly accessible) information on the relative diffusional resistances of constituent layers of composite NF membranes. Lemordant et al. has also attempted to interpret the results of measurements of steady-state membrane potential in terms of fixed charge density within the membrane active layer. However, that estimate involved an arbitrary assump-

* Corresponding author. Tel.: +43-316-3805443; fax: +43-316-3809850.
E-mail address: andriy.yaroshchuk@kfunigraz.ac.at (A.E. Yaroshchuk).

tion about the ratio of diffusional resistances of membrane active layer and support.

Those and similar difficulties in the interpretation of conventional electrochemical and/or electrokinetic measurements with NF membranes are caused by their multilayer structure. The membranes consist of relatively thin active (or skin) layers responsible for separations and of supports reinforcing the membranes mechanically. In the conditions of steady state NF, supports do not directly influence the solute rejections [18]. However, other transport measurements are essentially influenced by the presence of supports. The most obvious examples are the electrical and diffusional resistances of membranes. Only the resistances of a series connection of active layer and support can be measured while the information on the active layer resistances is needed. Other examples are the measurements of electroosmosis or streaming potential where the presence of supports causes an internal concentrational polarisation whose extent is unknown because of the lack of information on the ratio of diffusional resistances of active layers and supports. Finally, in the measurements of membrane potential and osmosis an external composition difference is distributed in an unknown proportion between the active layers and supports. Various options are schematically illustrated in Fig. 1.

This problem has a quite fundamental nature. Under linear conditions only average membrane transport properties can be obtained from steady-state measurements. Information on the properties of constituent layers can be obtained from non-steady-state and/or non-linear measurements, alone. In this paper we shall explore the opportunities offered by non-steady-state techniques. Even in the simplest case of binary electrolyte solutions there are six independent phenomenological coefficients characterising each layer. We shall concentrate our attention on these two properties that are directly related to the fixed electric charge density in the active layer: the ion transport numbers and electrokinetic charge density. Notably, those two parameters may yield essentially different information [19].

To correctly select the non-steady-state techniques for the studies of transport properties of active layers it is important to have an idea of characteristic times of establishment of a steady state. If the shortest time for which a measurement is still technically possible turns out to be longer than that

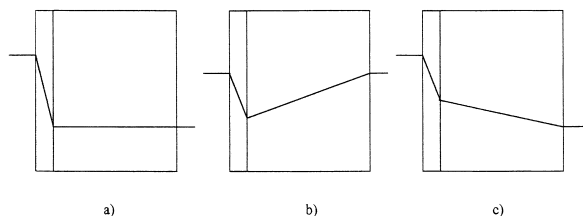


Fig. 1. Schematic concentration profiles inside a composite membrane: (a) mode of charged chemical capacitors (RO, NF); (b) no external concentration difference (electroosmosis, streaming potential); (c) applied external concentration difference (membrane potential, osmosis).

characteristic time the measurement is not informative since its results are controlled by the average membrane transport properties. In the results and discussion section it is shown that the characteristic relaxation time may be as short as several tens of milliseconds. At the same time it can be shown that for realistic test cells parameters concentration changes and volume flows cannot be observed at times shorter than a couple of seconds. Thus for instance, in AC electroosmosis the shortest times at which a reliable determination of electroosmotic pressure was still possible was not shorter than 1 s [20].

The only suitable response is electrical. Electrical capacities in electrolyte solutions charge very rapidly, namely, at characteristic times of diffusional relaxation of the diffuse part of double electric layer. Even in very dilute solutions that time does not exceed millionth parts of a second. Therefore, the electric current can always be considered continuous, which simplifies interpretations remarkably. At the same time, sufficiently rapid perturbations can be set up not only electrically but also hydraulically and chemically.

It has already been mentioned that the main problems in the interpretation of transport phenomena in multilayer membranes are the distribution of external composition difference between the constituent layers and/or the concentrational polarisation of boundaries between them. The latter gives rise to the appearance of diffusional components of electric potential difference even if there is no external composition difference. The concentrational polarisation makes impossible, e.g. an immediate determination of streaming potential coefficient of active layer from the measurements of steady-state streaming potential. To account for the polarisation one needs to know the ratios of diffusional resistances of constituent layers as well as some of their transport properties (e.g. ion transport numbers), which, properly speaking, are sought-for values. However, the concentrational polarisation cannot develop immediately. It is shown below that the passage of electric current and/or volume flow across a boundary between layers with different transport properties makes that boundary a source of salt flow. The cause for a time lag is the fact that this flow has to charge the distributed chemical capacity [18] of a vicinity of the boundary to an extent before the salt chemical potential there changes appreciably. Only after that there arise noticeable deviations of salt chemical potential from the initial value, and there appears a diffusional component in the electrical response.

Strictly speaking, inside multilayer membranes there arise local gradients of not only solution composition but also of hydrostatic pressure (even if the external pressure difference is zero). That somewhat complicates the interpretation of measurements carried out at zero or given hydrostatic pressure difference.¹ However, fortunately, the transport properties of membranes defined at zero

¹ Due to the slow hydraulic relaxation the most of 'rapid' measurements are performed just in this mode.

hydrostatic pressure difference and at zero volume flow usually differ only slightly. The appearance of internal hydrostatic pressure differences can, evidently, bring about only variations in transport properties confined between those two limiting modes. Therefore, further on we shall neglect the influence of hydraulic conditions. In effect, this means that we shall consider all the phenomena at a given (in particular, zero) transmembrane volume flow. In this context one should also mention that the distributed hydraulic capacity within the membrane phase most probably is negligibly small. Therefore the internal hydrostatic pressure gradients establish themselves almost instantly and do not cause any phase shift. The principal source of non-trivial non-steady-state phenomena is the concentrational polarisation of boundaries between layers with different transport properties (including the external membrane boundaries).

2. Theory

As the starting point we use the equation of non-steady state diffusion. As such it is well known and does not need to be derived. However, we are going to use its phenomenological form featuring the salt chemical potential instead of its concentration. In this case taking into account the species conservation is somewhat non-trivial. Besides that in binary electrolyte solutions there also is a non-trivial point of turning from diffusion of ions to that of a salt.

First, let us derive an expression for the local ionic fluxes in a binary electrolyte in terms of electric current and salt chemical potential. As the starting point we use this relationship (derived in the approximation of no direct coupling between ionic fluxes [19]) between the ionic fluxes and the gradients of their electrochemical potentials, μ_i^e :

$$j_i = -\frac{gt_i}{(FZ_i)^2} \frac{\partial \mu_i^e}{\partial x} + j_v c_i \tau_i \quad (1)$$

where g is the membrane electric conductivity, t_i are the ionic transport numbers in the membrane, Z_i are the ionic charges, F is the Faraday constant, c_i are the virtual ionic concentrations (the concentrations in the solution that could be in thermodynamic equilibrium with a given point inside the membrane [19]), j_v is the transmembrane volume flow density and τ_i are the so called ionic entrainment coefficients. They are formally defined as the proportionality coefficients between the ion fluxes scaled on their concentrations and the volume flow at zero transmembrane electrochemical potential difference for a given ion. The ionic entrainment coefficients cannot be directly measured. However, the irreversible thermodynamics makes possible their calculation proceeding from measurable quantities.

By using this definition of electric current density:

$$I \equiv F \sum_i^n Z_i j_i \quad (2)$$

and this definition of electrochemical potential:

$$\mu_i^e \equiv \mu_i + FZ_i \phi \quad (3)$$

where μ_i is the chemical potential and ϕ is the electrical potential, we can obtain this expression for the electric potential difference:

$$\frac{\partial \phi}{\partial x} = -\frac{I}{g} - \frac{1}{F} \sum_i^n \frac{t_i}{Z_i} \frac{\partial \mu_i}{\partial x} + \frac{\rho}{g} j_v \quad (4)$$

where we have introduced the electrokinetic charge density:

$$\rho \equiv F \sum_i^n Z_i c_i \tau_i \quad (5)$$

By substituting this into Eq. (1) we obtain:

$$j_i = -\frac{g}{F^2} \frac{t_i}{Z_i} \left(\frac{1}{Z_i} \frac{\partial \mu_i}{\partial x} - \sum_j^n \frac{t_j}{Z_j} \frac{\partial \mu_j}{\partial x} \right) + j_v c_i T_i + \frac{I t_i}{F Z_i} \quad (6)$$

where we have introduced the ionic entrainment coefficients at zero electric current:

$$T_i \equiv \tau_i + \frac{\rho t_i}{F Z_i c_i} \quad (7)$$

In the case of binary electrolytes (single salts)

$$\frac{\partial \mu_i}{\partial x} = \frac{1}{\nu_1 + \nu_2} \frac{\partial \mu}{\partial x},$$

where μ is the salt chemical potential, and ν_1, ν_2 are the ion stoichiometric coefficients. It is easy to show that in this case the ionic entrainment coefficients at zero electric current are equal for cations and anions so only one for the salt can be introduced:

$$T_1 \equiv T_2 \equiv T_s \equiv \tau_1 t_2 + \tau_2 t_1 \quad (8)$$

Thus, finally Eq. (6) for ionic fluxes takes this form:

$$j_i = \nu_i \left[-\chi \frac{\partial \mu}{\partial x} + j_v c_s T_s \right] + \frac{I t_i}{F Z_i} \quad (9)$$

where we have introduced the membrane diffusional permeability for the salt in this way:

$$\chi \equiv \frac{g t_1 t_2}{(F Z_1 \nu_1)^2} \quad (10)$$

Expectedly, at zero electric current the fluxes of cations and anions are stoichiometric, and one can easily introduce the salt flux by dividing either of ion fluxes by the corresponding stoichiometric coefficient. If the electric current is non-zero introducing the transmembrane salt flux in a unique way becomes rather tricky. The point is that ions come to reservoirs not only through the membrane but also from electrodes. Generally, the flux of a neutral salt cannot be introduced

without accounting for the contribution of electrodes. One of the options of taking it into account implicitly is to assume that the electrodes are reversible with respect to only one of ions [21]. Then the accumulation of another ion in a reservoir is caused exclusively by its transmembrane transfer. Let the electrode be reversible to the ion ‘2’, and the salt flux be defined by $j_s \equiv j_1/v_1$.

In a one-dimensional non-steady-state diffusion the spatial change of the solute flux within an infinitely thin layer is equal to the rate of accumulation of this solute in the same layer. For the local ion flux densities we use Eq. (9). From the definition of salt permeability of Eq. (10) it is seen that whichever of ion transport numbers is small so does the salt permeability. One of ion transport numbers is always small, e.g. in ion-exchange media in equilibrium with relatively dilute electrolyte solutions.

For the salt accumulation of fundamental importance are the ion distribution coefficients. In the state of local thermodynamic equilibrium the local ion concentrations can be represented in this way:

$$c_i = c_s v_i \Gamma_i \quad (11)$$

As there is no accumulation of electric charge anywhere within the membrane² cations and anions are added to (or withdrawn from) an infinitely thin membrane layer in stoichiometric quantities. Therefore the local variation of salt amount per unit volume can be estimated for any of ions:

$$\delta q_s \equiv \frac{\delta c_i}{v_i} = \delta c_s \left(\Gamma_i + c_s \frac{d\Gamma_i}{dc_s} \right) \quad (12)$$

The specific chemical capacity is defined this way:

$$\alpha \equiv \left(\frac{\partial q_s}{\partial \mu} \right)_{T,P} \quad (13)$$

For ideal solutions by using Eqs. (12) and (13) we obtain:

$$\alpha = \frac{c_s}{RT} \left(\Gamma_i + c_s \frac{d\Gamma_i}{dc_s} \right) \quad (14)$$

In ion-exchange media in equilibrium with dilute electrolyte solutions the distribution coefficient of coions is small.³ The second term in parenthesis in Eq. (14) can be shown to be of the same order of magnitude as the first one. Therefore the specific chemical capacity of ion-exchangers is essentially smaller than that of bulk electrolyte solutions (the latter is evidently equal to c_s/RT). Since cations and anions are added to (or withdrawn from) a layer in stoichiometric quantities the conservation law can be applied to either of

them. Thus, the one-dimensional equation of salt conservation looks this way:

$$\frac{\partial}{\partial x} \left(\frac{j_i}{v_i} \right) \equiv \frac{\partial j_s}{\partial x} = - \frac{\partial q_s}{\partial t} \quad (15)$$

By substituting Eqs. (9) and (12) into it and accounting for the conservation of electric current density and volume flow we finally obtain:

$$\alpha_k \frac{\partial \mu}{\partial t} = \chi_k \frac{\partial^2 \mu}{\partial x^2} + j_v \frac{\partial}{\partial x} \left(c_s T_s^{(k)} \right) + \frac{I}{FZ_i} \frac{\partial t_i^{(k)}}{\partial x} \quad (16)$$

where α_k is the specific chemical capacity of k th layer and χ_k is its specific diffusional permeability, $T_s^{(k)}$ is its salt entrainment coefficient and $t_i^{(k)}$ is the transport number of i th ion there. We consider the deviations of salt chemical potential from its equilibrium value small so Eq. (16) is a linear differential equation in partial derivatives. If each layer is macroscopically homogeneous the coefficients in Eq. (16) are simply layer-specific constants. Accordingly, the last term in right-hand side of Eq. (16) is equal to zero within each of them. The second term can be shown to be of the second order of magnitude in small j_v (or of the order of magnitude of $j_v I$, which is the same if both of them are small). Therefore in the linear approximation it can also be neglected.⁴ Thus, in dimensionless form Eq. (16) reads this way:

$$\beta_k \frac{\partial \mu}{\partial \tau} = \frac{\partial^2 \mu}{\partial \xi^2} \quad (17)$$

where we have scaled the transmembrane co-ordinate on the active layer thickness, $\xi \equiv x/l_a$, and time on the diffusion relaxation time of active layer defined in this way:

$$t_0 \equiv \frac{\alpha_a}{\chi_a} l_a^2 \quad (18)$$

Index ‘a’ denotes the properties of active layer. Coefficients β_i are defined in this way:

$$\beta_k^2 \equiv \frac{\alpha_k \chi_a}{\alpha_a \chi_k} \quad (19)$$

By definition $\beta_a \equiv 1$.

One of boundary conditions is that of continuity of salt chemical potential (local interfacial equilibrium). The boundary condition for the salt flux needs a special consideration. The spatial derivatives of salt entrainment coefficient and of ion transport number become infinite at the layer boundaries if there are step-wise changes in those properties. Accordingly, the salt flux undergoes a jump whose magnitude is proportional to the changes in those properties as well as to the volume flux and/or electric current density:

$$\begin{aligned} & \chi_k \left. \frac{\partial \mu}{\partial \xi} \right|_{\xi=\xi_k} - \chi_{k+1} \left. \frac{\partial \mu}{\partial \xi} \right|_{\xi=\xi_k} \\ &= l_a \left(j_v c_s \Delta T_s \Big|_{\xi=\xi_k} + \frac{I}{FZ_1 v_1} \Delta t_1 \Big|_{\xi=\xi_k} \right) \end{aligned} \quad (20)$$

² Remember that we consider the times much longer than the characteristic Maxwell–Wagner relaxation time. Therefore even under non-steady-state conditions the electric current is continuous.

³ For counterions the distribution coefficient is large. However, the second term in parenthesis is negative in this case and can be shown to compensate the first one almost exactly.

⁴ Nevertheless both terms contribute to boundary conditions (see below).

where ξ_k are the co-ordinates of the boundaries, $\Delta T_s \equiv T_s|_{\xi_k-0} - T_s|_{\xi_k+0}$, $\Delta t_1 \equiv t_1|_{\xi_k-0} - t_1|_{\xi_k+0}$ are the changes of corresponding properties at the boundary. Evidently, if both electric current and volume flow are zero, the salt flux is continuous at all boundaries. If either of them is non-zero, the boundaries with changes in corresponding transport properties become sources of salt flux. Despite the appearance of salt flux sources electric charges do not arise at the boundaries. It is easy to show that exactly as much charge is taken away from a boundary by anions as it is brought to it by cations and vice versa. The initial conditions depend on the way the system is disturbed from equilibrium.

The purpose of this paper is to discuss the potentialities of non-steady-state techniques without going into too much detail. Therefore we shall mainly consider the simplest system where the phenomena of interest already manifest themselves. Namely, we mainly consider an active layer confined by identical semi-infinite media from both sides. Thus, we neglect the differences in properties between membrane supports and free electrolyte solutions. If the supports do not have either electrochemical or osmotic activity their identification with free electrolyte solutions does not bring about any qualitative changes in the system behaviour. At least some of supports are coarse-porous media with up to 80% of water. Therefore even the quantitative differences may be rather small.

As discussed above only the electrical response of the system can easily be observed at short times. However, a perturbation can be set up in any of these three ways: by changing the salt concentration, the hydrostatic pressure or by applying a voltage difference. Accordingly, we shall consider the transient membrane potential, the transient filtration potential and the electrical impedance. In either case the temporal evolution of electrical response is tracked.

The solution to Eq. (17) is always sought in this form:

$$\mu_i(\xi, \tau) \equiv \frac{1}{2\pi} \exp(-i\omega\tau) f_i(\xi, \omega) \quad (21)$$

where ω is the dimensionless circular frequency (scaled on $1/t_0$), $f_i(\xi, \omega)$ is the complex spectral density of temporal response. By substituting Eq. (21) into Eq. (17) we obtain these fundamental solutions:

$$f_i^{(\pm)}(\xi, \omega) \equiv \exp\left(\pm(1-i)\beta_i\sqrt{\frac{\omega}{2}}\xi\right) \quad (22)$$

Accordingly, the general solutions for the spectral densities have this form:

$$f_i(\xi, \omega) = A_i^{(+)} \exp\left((1-i)\beta_i\sqrt{\frac{\omega}{2}}\xi\right) + A_i^{(-)} \exp\left(-(1-i)\beta_i\sqrt{\frac{\omega}{2}}\xi\right) \quad (23)$$

where $A_i^{(\pm)}$ are the integration constants.

2.1. Transient membrane potential

The concentration jump at the active membrane surface can be set up by the dab technique (see Section 3 for the description of principle of this technique). Two electrolyte solutions of different concentrations are brought into (ideally) immediate contact across a membrane being preliminary equilibrated with one of them. Thus, a stepwise change of salt concentration is created at the active membrane surface. If the semi-infinite electrolyte solution bordering the active membrane surface is assumed to be unstirred this corresponds to a step-wise chemical potential change at one of infinities (for definiteness let it be $-\infty$). Initially, the most of applied composition difference is usually located within the active layer, and the electric response is controlled by its transport numbers, which makes possible their direct determination.

In the unstirred half-space to the left from the membrane active surface a stepwise concentration jump at any frequency is given at $-\infty$. Therefore $A_l^{(-)} = 0$. For the other integration constants from the conditions of continuity of salt chemical potential and flux at the boundaries as well as from the boundedness of solution at $+\infty$ we obtain this system of linear algebraic equations:

$$\begin{aligned} A_l^{(+)} - A_a^{(+)} - A_a^{(-)} &= -F(\omega) \\ rA_l^{(+)} - A_a^{(+)} + A_a^{(-)} &= 0 \\ A_a^{(+)}y(\omega)^{-1} + A_a^{(-)}y(\omega) - A_r^{(-)} &= 0 \\ A_a^{(+)}y(\omega)^{-1} - A_a^{(-)}y(\omega) + r_rA_r^{(-)} &= 0 \end{aligned} \quad (24)$$

where we have introduced these notations:

$$y(\omega) \equiv \exp\left(- (1-i)\sqrt{\frac{\omega}{2}}\right) \quad (25)$$

$$r \equiv \sqrt{\frac{\alpha_s\chi_s}{\alpha_a\chi_a}} \quad (26)$$

$$F(\omega) \equiv \pi\delta(\omega) + \frac{i}{\omega} \quad (27)$$

is the Fourier-transform of unit-step function.⁵ Indices 'l' and 'r' denote the left and right half-spaces, the index 'a' denotes the active layer, and the index 's' does the properties of both half-spaces confining the active layer (remember that we consider them identical). We are looking for the chemical potential difference across the active layer. Its spectral density is equal to:

$$Q(\omega) \equiv f_a(1, \omega) - f_a(0, \omega) \equiv A_a^{(+)}\left(y(\omega)^{-1} - 1\right) + A_a^{(-)}\left(y(\omega) - 1\right) \quad (28)$$

⁵ In the linear mode the response is directly proportional to the perturbation. Therefore the amplitude of the latter can be chosen equal to unity without any loss of generality.

By solving the system of Eq. (24) we obtain this:

$$Q(\omega) = F(\omega) \frac{r}{r + \coth\left(\frac{1-i}{2}\sqrt{\frac{\omega}{2}}\right)} \quad (29)$$

The temporal response is obtained through inverse Fourier transform:

$$\begin{aligned} \Delta\mu_a(\tau) &\equiv \mu_a(1, \tau) - \mu_a(0, \tau) \\ &= \frac{1}{2\pi} \int_{-\infty}^{+\infty} d\omega Q(\omega) \exp(-i\omega\tau) \end{aligned} \quad (30)$$

The response of interest is given by the real part of Eq. (30).

It can be shown that the electric potential difference arising due to the concentration gradients is independent of the shape of concentration profile within each layer and, thus, is controlled only by the distribution of applied concentration difference between the active layer and the adjacent half-spaces [22–24]. Therefore, the electric potential difference is related to the salt chemical potential difference located on the active layer, $\Delta\mu^{(a)}$ this way:

$$\Delta\phi_m(\tau) = \left(t_1^{(a)} - t_1^{(s)}\right) \Delta\mu_a(\tau) + \left(t_1^{(s)} - \frac{v_2}{v_1 + v_2}\right) \quad (31)$$

where we have taken into account that the applied salt chemical potential difference is assumed to have a unit magnitude. In the particular case of KCl solutions where

$$t_1^{(s)} \approx \frac{v_2}{v_1 + v_2} = 1/2$$

the second term disappears.

2.2. Transient filtration potential

A transmembrane volume flow is assumed to be set up stepwise. Though technically that is not easy (see below for some discussion on that) a Fourier analysis of electrical response allows to account for the deviations from an immediate increase in volume flow.

Since we consider both the half-spaces adjacent to the active layer identical, the problem has a mirror symmetry about the middle of it. Therefore there are only two independent integration constants. For their determination we obtain this system of equations:

$$\begin{aligned} A_a \left(\frac{1}{\sqrt{y(\omega)}} - \sqrt{y(\omega)} \right) - A_s &= 0 \\ A_a \left(\frac{1}{\sqrt{y(\omega)}} + \sqrt{y(\omega)} \right) + rA_s &= S(\omega) \end{aligned} \quad (32)$$

where we have introduced a source function, $S(\omega)$, that in this case has this form:

$$S(\omega) \equiv j_v(\omega) c_s \Delta T_s \left(\frac{l_a}{\chi_a} \right) \frac{1+i}{\sqrt{2}\omega} \quad (33)$$

Here $j_v(\omega)$ is the Fourier transform of applied volume flow (e.g. the Fourier transform of unit step function given by Eq. (27)).

The system of Eq. (33) is easy to solve to yield this for the spectral density of salt chemical potential difference across the active layer:

$$R(\omega) = \frac{2S(\omega)}{r + \coth\left(\frac{1-i}{2}\sqrt{\frac{\omega}{2}}\right)} \quad (34)$$

At $\omega \rightarrow \infty$ (very short observation times) the response function $R(\omega)$ evidently goes to zero, which just confirms the feeling that immediately after the set-up of volume flow there is no concentrational polarisation at the active layer boundaries. To pass from the salt chemical potential difference to the measurable voltage difference we should specify the location (and, generally, the nature) of measuring electrodes. At any finite frequency the zones where the salt chemical potential deviates from its equilibrium value have finite dimensions. We assume that both measuring electrodes are always located outside those zones, i.e. in solutions with equilibrium concentrations. Accordingly, whatever the nature of those reversible electrodes there arise no electrode voltage difference between them. On the other hand, there are chemical potential differences between each of electrodes and the corresponding active layer surface. Their sum is equal to the chemical potential difference across the active layer in magnitude and has the opposite sign. The chemical potential differences in the adjacent solutions also make a contribution into the diffusional component of electric potential difference, which reads this way:

$$\Delta\phi_d = j_v(\omega) c_s \Delta T_s \Delta t_1 \left(\frac{l_a}{\chi_a} \right) \sqrt{\frac{2}{\omega}} \frac{1+i}{r + \coth\left(\frac{1-i}{2}\sqrt{\frac{\omega}{2}}\right)} \quad (35)$$

The electrical response is evidently given by Eq. (35) plus a streaming potential contribution, which establishes itself immediately and, thus, does not give rise to any phase shift between the volume flow and the electric potential difference. Though the streaming potential is of a central interest from the viewpoint of membrane characterisation its role is trivial in this context, so we shall concentrate our attention on the diffusional contribution given by Eq. (35).

2.3. Electrical impedance

The system can also be deviated from equilibrium electrically. In this case creating a harmonic perturbation is much easier than in the case of a hydraulic perturbation. If the voltage response to a given harmonic current is measured the system electrical impedance can be obtained. However, studying the electrical response to a step-wise change in electric current may be even more informative. In any case,

from the boundary condition of Eq. (20) it is seen that electrical and hydraulic perturbations have the same effect on the evolution of salt chemical potential profile. Accordingly, the spectral density given by Eq. (34) applies to this case, too, with the only difference being a somewhat other form of source function:

$$S(\omega) \equiv \frac{I(\omega)}{FZ_1\nu_1} \Delta t_1 \left(\frac{l_a}{\chi_a} \right) \frac{1+i}{\sqrt{2\omega}} \quad (36)$$

In the case of a harmonic current, $I(\omega)$ is simply a constant. In other cases it is a Fourier transform of the applied current. By reasoning in exactly the same way as above we can pass from the chemical potential difference across the active layer to the electric potential difference measured with a pair of reversible electrodes located outside the zones where the concentration changes:

$$\Delta\phi_d = \frac{I(\omega)}{(FZ_1\nu_1)^2} (\Delta t_1)^2 \left(\frac{l_a}{\chi_a} \right) \sqrt{\frac{2}{\omega}} \frac{1+i}{r + \coth\left(\frac{1-i}{2}\sqrt{\frac{\omega}{2}}\right)} \quad (37)$$

Similarly to the previously discussed case there also is an immediate component of electric potential difference, namely the Ohmic voltage drop. However, in the case of transient filtration potential the steaming potential and the diffusion potential components are thermodynamically independent, while in the case under consideration the part of Ohmic voltage drop located within the active layer is controlled by the same active layer transport properties as the diffusional component. Since our ultimate goal is to figure out in what way those properties can be obtained from experimental data we should explicitly include this part of Ohmic voltage drop into consideration. The experimentally measured voltage drop evidently includes the contributions of solution layers between the membrane surfaces and measuring electrodes. However, they can be easily excluded through calibration measurements carried out without the membrane. Therefore we do not include them into this expression for the total voltage drop:

$$z(\omega) \equiv \frac{\Delta\phi(\omega)}{I(\omega)} = \frac{l_s}{g_s} + \frac{l_a}{g_a} \times \left(1 + \frac{(t_1^{(a)} - t_1^{(s)})^2}{t_1^{(a)}(1 - t_1^{(a)})} \sqrt{\frac{2}{\omega}} \frac{1+i}{r + \coth\left(\frac{1-i}{2}\sqrt{\frac{\omega}{2}}\right)} \right) \quad (38)$$

where l_s and g_s are the thickness and specific electric conductivity of support, and we have used Eq. (10) to express the active layer diffusional permeability through its electric conductivity and ion transport numbers.

3. Results and discussion

3.1. Estimates of relaxation time

It is well known that the characteristic time of the propagation of a one-dimensional ‘diffusional front’ up to the distance l into a homogeneous half-space after a sudden change in the solute concentration at its boundary can be estimated as l^2/D where D is the solute diffusion coefficient. It should be stressed that this estimate relates to homogeneous media where the chemical (diffusional) resistance and chemical capacity of the same medium control the process. A model-independent expression for the characteristic time is given by Eq. (18).⁶ The crucial point is that the specific chemical capacity and permeability of the same medium appear in it. This characteristic time estimated for the active layers of NF membranes may be very short. It could be quite difficult to create sudden concentration or volume flow changes within still shorter periods of time. Fortunately, we deal with an inhomogeneous medium. A thin and relatively dense active layer is followed by a much looser and thicker support. Thus, we deal with diffusion through a relatively large chemical resistance into a relatively large chemical capacity. From electrical engineering it is known that in such situations the relaxation time (which roughly is the product of a resistance and a capacity) is controlled by the largest resistance and the largest capacity in the system. Therefore the characteristic relaxation time may be essentially longer than that given by Eq. (18). It can be roughly estimated in this way. Let us suppose that the solute concentration is suddenly changed at the surface of active layer. Within a period of time as short as t_0 an almost linear chemical potential profile is established within it. Therefore the solute flow density across it can be estimated as

$$J_s \sim \frac{\chi_a}{l_a} \delta\mu \quad (39)$$

where $\delta\mu$ is the deviation of chemical potential from the initial value. We are interested in the deviations from the initial value of the chemical potential of the boundary between the active layer and support. This value remains almost unchanged until the chemical capacity of adjacent part of support is noticeably charged. The dimension of this part can be estimated in this way. In a quasi-steady state the differences of chemical potential are equally distributed among layers having the same diffusional permeabilities. Therefore the value of chemical potential at the boundary between the active layer and the support is about half-way between its original and final values when the diffusional resistance of the part of support already encompassed by

⁶ It is easy to show that it reduces to l_a^2/D_a within the scope of a simple model and remains of the same order of magnitude for more sophisticated ones.

the chemical potential change is as large as that of active layer. Its thickness, l_r , can be estimated in this way:

$$l_r \sim l_a \frac{\chi_s}{\chi_a} \quad (40)$$

The chemical capacity (per unit area) of such a layer is equal to $\alpha_s l_r$. The time needed for the flux of Eq. (39) to change the chemical charge of this capacity in $\delta\mu$ is evidently equal to

$$t_{ch} \sim \frac{\alpha_s l_r \delta\mu}{J_s} = \alpha_s \chi_s \left(\frac{l_a}{\chi_a} \right)^2 \quad (41)$$

The dimensionless characteristic relaxation time is

$$\tau_{ch} \equiv \frac{t_{ch}}{t_0} = \frac{\alpha_s \chi_s}{\alpha_a \chi_a} \equiv r^2 \quad (42)$$

As both the chemical capacity and the diffusional permeability of support may be essentially larger than that of active layer the dimensionless characteristic relaxation time may be noticeably larger than unity. The same characteristic relaxation time is obtained if one assumes a sudden appearance of salt flux sources at the active layer surfaces due to the passage of either electric current or volume flow through the membrane.

For a simple model of a homogeneous ion-exchanger Eq. (41) can be rewritten this way:

$$t_{ch} \sim D_s \left(\frac{l_a}{D_a \Gamma_a} \right)^2 \quad (43)$$

Here D_a and D_s are the salt diffusion coefficients within the active layer and the support, respectively, Γ_a is the salt (coion) distribution coefficient in the active layer. By taking $l_a = 0.2 \mu\text{m}$, $D_a = 10^{-6} \text{ cm}^2/\text{s}$, $D_s = 3 \times 10^{-6} \text{ cm}^2/\text{s}$ and $\Gamma_a = 0.2$ as values characteristic of nanofiltration membranes we obtain $t_{ch} \approx 0.03 \text{ s}$.

3.2. Transient membrane potential

Fig. 2 shows the results of numerical Fourier transform of the spectra given by Eq. (29). A very rapid initial relaxation turns into a much slower decay so logarithmic scale

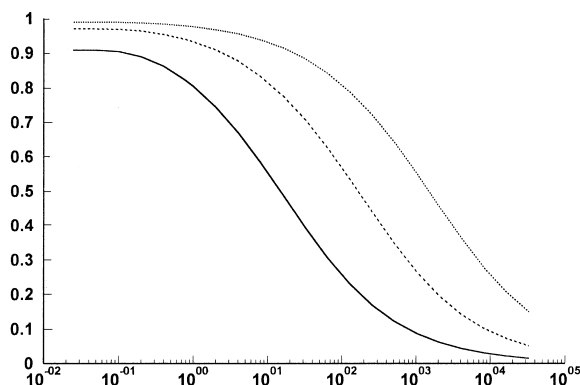


Fig. 2. Dab technique: chemical potential difference across active layer against dimensionless time: $r=10$ (solid); $=33$ (dashed), $=100$ (dotted).

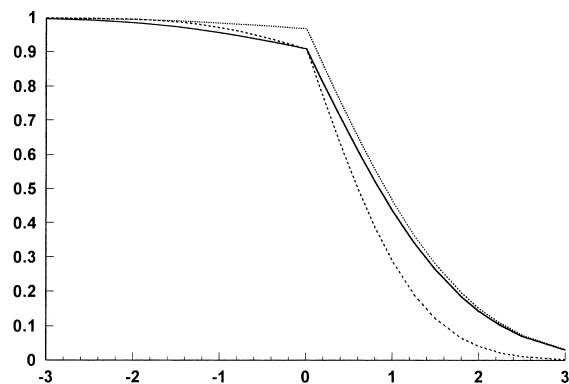


Fig. 3. Chemical potential profiles shortly after the contact between the membrane surface and the switch tip: $\beta_1=1$; $r_1=10$; $\tau=1$ (solid), $=0.5$ (dashed); $r_1=30$; $\tau=1$ (dotted).

had to be used. In this scale one can clearly see the plateaux where the initial membrane potential is observed followed by quasi-linear parts becoming concave down when the zero value is approached. The plots shown in Fig. 2 were calculated for various values of parameter r . It is seen that they all have almost identical shape and are simply shifted one with respect to another along the time axis. The extent of this shift is almost exactly equal to the square of the ratio of parameters r used to calculate each of them. Thus, the rough estimate of Eq. (42) proves quite accurate. Another feature of the plots in Fig. 2 is that they do not exactly approach unity at very short times. That can also be seen from Eq. (29) if we let frequency in it to increase toward infinity. The limiting value is $r/(r+1)$ which may be quite close to unity (especially for membranes with relatively dense active layers) but not exactly equal to it, nonetheless. Physically this means that the given chemical potential difference is distributed between the active layer and the adjacent solution immediately upon the contact (see Fig. 3). Fortunately, the most of it is located in the denser of two phases, i.e. in the active layer. Accordingly, the initial membrane potential is probably only slightly underestimated in most cases. Nevertheless, this fact should be born in mind, and may explain some features of experimental data as discussed below.

Fig. 4 shows some of chronopotentiogrammes obtained for PES10 membrane (Kalle, Germany) at relatively short times (up to 1 s) with the dab technique. The experimental details are described elsewhere [25]. The idea of dab technique is to equilibrate a membrane with an electrolyte solution and let it be in contact with it from one side only (typically that is the support side). The active side of the membrane is suddenly touched with a hanging drop of solution of a different concentration, and the electrical response to this is tracked.

Though at very short times some fluctuations have been observed the general run of the plots is quite similar to the theoretically predicted. In the logarithmic scale a kind of plateau is followed by an almost linear decay. Notably, the relaxation time becomes longer with the decreasing base

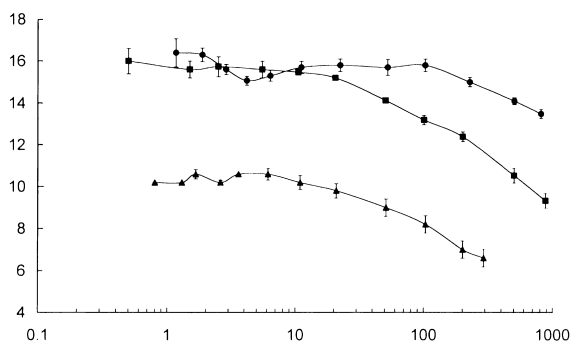


Fig. 4. Transient membrane potential (mV) measured for PES10 membrane in KCl solutions against time (in ms), base concentration: 0.001 M (●), 0.01 M (■), 0.1 M (▲); $c'/c'' = 2$.

concentration. That is especially visible for the change from 0.01 to 0.001 M base solution: the relaxation time becomes almost an order of magnitude longer. That is quite consistent with the hypothesis that the active layers of PES10 membranes have pronounced electrochemical activity in relatively dilute solutions (for other indications see below). Indeed, both the chemical capacity and diffusional permeability of ion-exchangers decrease with decreasing electrolyte concentration. That gives rise to an increase in the characteristic relaxation time in accordance with Eq. (41). The decrease in the relaxation time with the change in base concentration from 0.01 to 0.1 M was less pronounced because here the electrochemical activity of membrane was lower and, accordingly, the dependence of its transport and accumulation properties on the salt concentration became weaker. The same behaviour occurred for all the ratios of higher to lower concentrations studied.

The ion transport numbers within active layer have been estimated in conventional way, namely we considered the chemical potential difference small and took the transport numbers out of the integral in the Henderson's formula. In this way we obtained:

$$\Delta\varphi_m = \frac{RT}{F} (2t_+ - 1) \ln \left(\frac{a''}{a'} \right) \quad (44)$$

where a' , a'' are the solution activities. Eq. (44) assumes the ion transport numbers to be independent of solution concentration within the range between c' and c'' . The validity of this assumption is usually checked in this way. The membrane potential is plotted against the natural logarithm of ratio of activities. If the resulting plot proves a straight line passing through the origin the assumption is valid, and the transport numbers can be obtained from the slope. Fig. 5 shows the experimental data presented in that way for PES10 membrane. It is seen that for the base concentration 0.001 M KCl the plot remains linear until as large concentration ratio as 10. Usually ion transport numbers are fairly independent of concentration if one of them is very close to unity. However from the slope of straight line for potassium ions we obtain the transport number of 0.96. The explanation

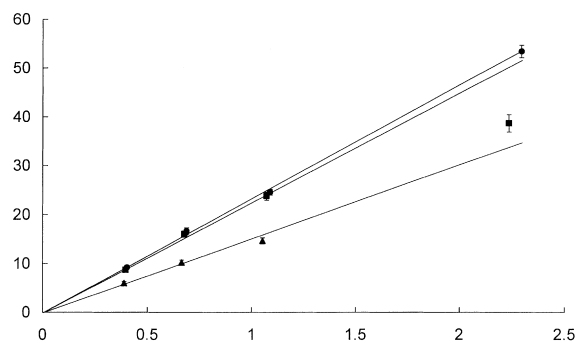


Fig. 5. Initial membrane potential (mV) measured for PES10 membrane against the natural logarithm of ratio of activities; base concentration: 0.001 M (●), 0.01 M (■), 0.1 M (▲).

of this fact is that a part of applied chemical potential difference was located outside the active layer as discussed above. Accordingly, the cation transport number was slightly underestimated. The actual transport number was probably very close to unity and, therefore, did not depend on the salt concentration. That interpretation is confirmed by the data obtained with higher base concentrations. Indeed, for the base concentration equal to 0.01 M the plot remains linear only until the concentration ratio of 3, and for the base concentration of 0.1 M even this ratio proves too large for the plot to keep the linearity. Remarkably, the linear part of the plot for 0.01 M base concentration almost coincides with that obtained with the 0.001 M base solution. Hence, even in this solution the cation transport number could be fairly close to unity, and the deviation in the slope from the Nernstian one was probably caused by the just discussed phenomenon of distribution of applied difference of chemical potentials. As the diffusional permeability and chemical capacity of active layer increase with base concentration a somewhat larger part of chemical potential was located outside the active layer in this case. Accordingly the cation transport number was underestimated to a larger extent.

It is interesting to compare the transport numbers of potassium ions obtained from the initial membrane potential with the conventional average transport numbers determined from steady-state measurements performed by Koter [26]. Table 1 shows several representative values. It is seen that the average potassium transport numbers are essentially closer to 0.5 than the 'initial' ones. That means that the support does make a considerable contribution into the membrane diffusional resistance. Its relative contribution is especially large in the more concentrated solution. That is

Table 1
Summary of transport properties of PES10 membrane

Base concentration (KCl)	$t_1^{(a)}$	\bar{t}_1	$\left(\frac{I_s}{X_s} \right) \left(\frac{X_a}{I_a} \right)$
10^{-3} M	0.96	0.71	1.2
10^{-2} M	0.94	0.53	14.2
10^{-1} M	0.80	–	–

quite consistent with the hypothesis about an electrochemically active skin layer whose diffusional resistance strongly decreases with electrolyte concentration thus making the relative contribution of electrochemically passive support larger. Thus, the conventional steady-state membrane potential measurements may dramatically underestimate the active layer electrochemical activity.

3.3. Transient filtration potential

In the case of transient filtration potential, initially the internal concentrational polarisation does not have enough time to develop and to influence the electric response through the build-up of diffusion potential. Therefore, a streaming potential coefficient of active layer can be determined. The characteristic time of build-up of diffusion potential in this case is the same as the characteristic time of relaxation of initial membrane potential. However, the creation of a sufficiently steep pressure jump is technically more involved than the creation of a concentration jump. There are two main technical problems. The first one is the inevitable presence of hydraulic capacities in the high-pressure part of test cell. One of their principal sources may be the membrane deformation and/or membrane support compaction. Unfortunately, practically nothing is known about the related mechanical properties of NF membranes. Therefore, even a rough estimate of this kind of hydraulic capacity is impossible. Besides that there may also be other sources of considerable hydraulic capacity. Thus, the characteristic time of establishment of a steady hydrostatic pressure difference may essentially depend on the details of test cell design, and can realistically be estimated only experimentally. Unfortunately, we have not managed to complete the corresponding experiments, yet. However, a test cell has already been designed, and preliminary measurements are under way. Therefore the results may be available soon.

The second problem is just to perform a manipulation of opening or closing a valve or something similar in a sufficiently short time. The best valves we were able to find reportedly have the closing/opening time of around 0.005 s (supplied by Valcor, USA). That may be short enough, but we have not had an opportunity to try the valves, yet. Accordingly, one cannot be sure that they work that well in our specific experimental set-up.

Fortunately, at sufficiently short times there occurs an asymptotic behaviour of diffusion potential component that allows an extrapolation to zero time. Indeed, from Eq. (35) it is seen that if $\omega \rightarrow \infty$, the diffusional component of potential difference becomes inversely proportional to the square root of frequency. In time domain that means a direct proportionality to the square root of time. That is illustrated by Fig. 6. It is seen that with increasing parameter r the range of validity of the ‘root’ asymptotics becomes wider, which could be expected from the fact that the relaxation time becomes longer with it.

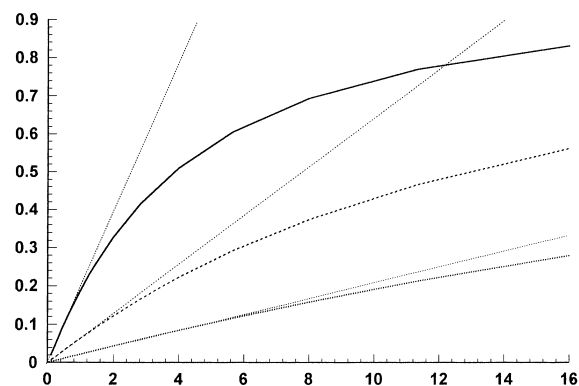


Fig. 6. Diffusional component of transient filtration potential (conditional units) against square root of dimensionless time: $r=10$ (solid), 33 (dashed), 100 (dotted).

Experimental data on transient filtration potential are available only for monolayer ion-exchange membranes [27]. Though they are not supported there always are unstirred layers near the membrane surfaces where concentrational polarisation can occur. For ion-exchange membranes the characteristic relaxation times are orders of magnitude longer than in the case of NF membranes. Therefore there have been practically no technical problems with the observations at short dimensionless times, and the ‘root’ asymptotics could be reliably identified and used for the extrapolation to zero time.

3.4. Electrical impedance

A general theoretical analysis of low-frequency electrical impedance of a multilayer membrane was carried out in [28,29]. We go on with a semi-quantitative analysis of the simplest system with two identical semi-infinite adjacent layers.

At sufficiently high frequencies⁷ the concentrational polarisation does not have enough time to develop. Accordingly, the diffusion-controlled imaginary part of impedance is close to zero. The same occurs at very low frequencies where the concentrational polarisation is fully developed, and voltage and current vary in phase. Thus, the imaginary part has an extremum. Fig. 7 shows examples of imaginary part of impedance spectra plotted against the square root of dimensionless frequency (in log scale). It is seen that variation of parameter r causes a simple shift of plots without any appreciable change in their shape. By using Eq. (38) it can be shown that the dimensionless circular frequency at which the imaginary part has the maximum is given by this equation:

$$\omega_m = \frac{2}{r^2} k \quad (45)$$

⁷ Here we are speaking about frequencies scaled on the characteristic frequency of diffusional relaxation. Of course, the frequencies high in this sense may still be (and typically are) quite low as compared with the frequencies typically employed in the most of impedance measurements.

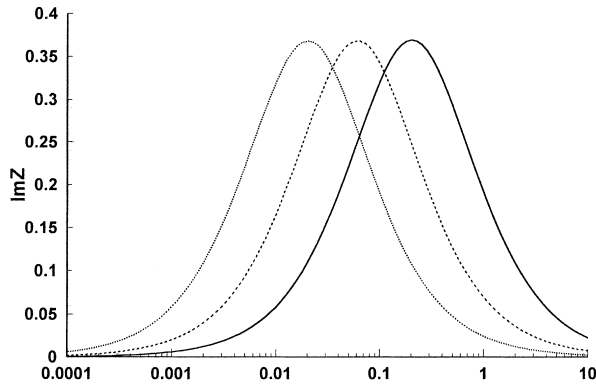


Fig. 7. Imaginary part of electrical impedance (scaled on l_a/g_a) of an active layer confined between two identical unstirred media against square root of dimensionless frequency: $t_1^{(a)} = 0.9$; $t_1^{(s)} = 0.5$; $r = 10$ (solid), 33 (dashed), 100 (dotted).

where k is practically independent of r if the latter is sufficiently large (e.g. it varies between 2.07 and 2 when r changes from 4 to 100). Therefore for the dimensional frequency at the point of maximum we obtain this:

$$\nu_m \approx \frac{2}{\pi} \frac{1}{t_{ch}} \quad (46)$$

where t_{ch} is given by Eq. (41). Thus, our rough estimate of characteristic relaxation time proves almost exact. From Eq. (38) it is also seen that the location of the maximum is not directly dependent on the ion transport number within active layer. At the same time its height proves almost independent of parameter r . It can be shown that when parameter r varies from 4 to 100 the height of maximum changes less than by 2%. The third useful finding is the fact that at sufficiently high dimensionless frequencies the imaginary part of impedance becomes independent of active layer thickness and is controlled mainly by the transport and accumulation properties of the phases adjacent to it. Indeed, if $\omega \rightarrow \infty$, and besides that $r \gg 1$ (which is often the case) from Eq. (38) we obtain this asymptotics:

$$\text{Im } z(\omega) \xrightarrow{\omega \rightarrow \infty} \frac{(t_1^{(a)} - t_1^{(s)})^2}{(FZ_1 \nu_1)^2} \frac{1}{\sqrt{\alpha_s \chi_s}} \frac{1}{\sqrt{\pi \nu}} \quad (47)$$

where ν is the dimensional frequency. The physics of disappearance of dependence on the active layer thickness is quite simple. The dimensions of zones where the chemical potential deviates from the initial value evidently decrease with frequency. At sufficiently high frequencies it proves much smaller than the active layer thickness. Here the concentrational polarisation of two interfaces occurs independently one from another.

The location of maximum, its height and the coefficient by the ‘root’ asymptotics of imaginary part of impedance, provide us with three equations for the determination of sought-for properties of active layer. Notably, its specific diffusional permeability, χ_a (or specific electric conductivity,

g_a) always appears in the same combination with its thickness, namely, (χ_a/l_a) (the absolute diffusional permeability of active layer). Therefore those two properties cannot be determined separately. At the same time, that diminishes the number of unknowns and enables us to consider the combination $\alpha_a \chi_s$ unknown, too. That is helpful since the transport and accumulation properties of membrane supports cannot be considered known. However, here it becomes evident that our model is too simplified for a quantitative comparison as it does not take into account the difference in transport and accumulation properties between the support and the electrolyte solution adjacent to the active layer. Accounting for that difference theoretically is relatively easy. Thus for instance, instead of asymptotics of Eq. (47) we obtain this one:

$$\text{Im } z(\omega) \xrightarrow{\omega \rightarrow \infty} \frac{(t_1^{(a)} - t_1^{(s)})^2}{(FZ_1 \nu_1)^2} \frac{1}{\sqrt{\pi \nu}} \frac{1}{2} \left(\frac{1}{\sqrt{\alpha_s \chi_s}} + \frac{1}{\sqrt{\alpha_w \chi_w}} \right) \quad (48)$$

where we used index ‘w’ to denote the properties of adjacent solution and reserved index ‘s’ for those of support. Moreover, an approximate solution very similar to Eq. (36) can be obtained in the limiting case of $r_w, r_s \gg 1$. It looks this way:

$$z(\omega) \equiv \frac{\Delta \phi(\omega)}{I(\omega)} = \frac{l_s}{g_s} + \frac{l_a}{g_a} \times \left(1 + \frac{(t_1^{(a)} - t_1^{(s)})^2}{t_1^{(a)}(1 - t_1^{(a)})} \sqrt{\frac{2}{\omega}} \frac{1+i}{\bar{r} + 2 \coth\left((1-i)\sqrt{\frac{\omega}{2}}\right)} \right) \quad (49)$$

where

$$\bar{r} \equiv \frac{2r_w r_s}{r_w + r_s}$$

This equation can be shown to have practically the same properties as Eq. (38) so the plots of imaginary part of impedance against the square root of frequency can be used in exactly the same way as discussed above. Thus for instance, for the location of maximum one can obtain this:

$$\nu_m \approx \frac{1}{2\pi} \left(\frac{\chi_a}{l_a} \right)^2 \left(\frac{1}{\sqrt{\alpha_w \chi_w}} + \frac{1}{\sqrt{\alpha_s \chi_s}} \right)^2 \quad (50)$$

The height of maximum is the same as in the case of symmetrical systems and is given by this

$$h_m \approx \frac{1}{(FZ_1 \nu_1)^2} \left(\frac{l_a}{\chi_a} \right) (t_1^{(a)} - t_1^{(s)})^2 f \quad (51)$$

where f is practically independent of \bar{r} and varies between 0.211 and 0.207 when \bar{r} changes from 4 to 100. The properties of support and adjacent electrolyte solution appear everywhere in the same combination, namely,

$$\left(\frac{1}{\sqrt{\alpha_w \chi_w}} + \frac{1}{\sqrt{\alpha_s \chi_s}} \right).$$

Therefore, we can consider it a single unknown, and that appears to make the number of equations equal to the number of unknowns.

Unfortunately, the equations prove to be not independent. Accordingly, to obtain the information on the active layer properties additional measurements are necessary. One of the options could be to determine directly the concentration changes caused by the passage of electric current. Of course, they cannot be measured inside the membrane. Therefore one cannot use harmonic currents of any appreciable frequency. A possibility is to polarise the membrane by direct current until a steady state is achieved. If the polarising electrodes are selected in a special way there is no concentration difference across the support in this state. Accordingly, by measuring the concentrations in the reservoirs separated by the membrane one can determine the chemical potential difference across the active layer. If the direct current is suddenly switched off, in the very first moment the chemical potential difference remains located within the active layer. As this difference is known from the independent measurements of concentrations the ion transport numbers can be directly determined from this initial value of e.m.f. Since after the switch-off the electric current is zero the electric potential difference can be measured by a pair of reversible electrodes located anywhere in each of reservoirs. It can be shown that the relaxation of potential difference in this case proceeds in a similar way to the build-up of diffusional component of filtration potential. In fact, the dependence is exactly the same if we consider the difference between the initial and actual values of membrane potential. Accordingly, the 'root' asymptotics is valid in this case, too, and the extrapolation to zero time should be possible. The additional advantage of this approach is that the interpretation is easily extendable to electrolyte mixtures (which is not the case for the conventional impedance spectroscopy). No experimental data of this kind are available to our knowledge. The closest results found in the literature are those on the 'relaxation of polarisation' in a cell with rotating ion-exchange membrane [30]. However, no direct determination of concentration has been attempted in this paper. Accordingly, the test cell design was quite different from that needed in the case of interest.

4. Conclusions

The ion transport numbers, electrokinetic charge density of active layers of NF membranes, in principle, can be obtained with a variety of non-steady-state techniques. However, the experimental studies in this field are still at their very beginning. Much more experimental effort is needed to really judge on the suitability of this or that technique. However, even at this stage one can see that each of them has its advantages and drawbacks. Therefore, the application of

several techniques to the same system is desirable for the minimisation of systematic errors.

Acknowledgements

One of the authors (A.Y.) is grateful to the Fonds zur Förderung der wissenschaftlichen Forschung (Austria) for financial support within the scope of Lisa-Meitner-Stipendium. Fruitful discussions with Dr E.K. Zholkovskij are gratefully acknowledged.

References

- [1] W.R. Bowen, H. Mukhtar, *J. Membr. Sci.* 112 (1996) 263.
- [2] W.R. Bowen, A.W. Mohammad, *Desalination* 117 (1998) 257.
- [3] W.R. Bowen, A.W. Mohammad, N. Hilal, *J. Membr. Sci.* 126 (1997) 91.
- [4] T. Tsuru, S. Nakao, S. Kimura, *J. Chem. Eng. Jpn.* 24 (1991) 511.
- [5] T. Tsuru, M. Urairi, S. Nakao, S. Kimura, *Desalination* 81 (1991) 219.
- [6] T. Tsuru, M. Urairi, S. Nakao, S. Kimura, *J. Chem. Eng. Jpn.* 24 (1991) 518.
- [7] X.L. Wang, T. Tsuru, S. Nakao, S. Kimura, *J. Membr. Sci.* 103 (1995) 117.
- [8] X.L. Wang, T. Tsuru, S. Nakao, S. Kimura, *J. Membr. Sci.* 135 (1997) 19.
- [9] X.L. Wang, et al. *J. Chem. Eng. Jpn.* 28 (1995) 186.
- [10] A.E. Childress, M. Elimelech, *J. Membr. Sci.* 119 (1996) 253.
- [11] M. Elimelech, W.H. Chen, J.J. Waypa, *Desalination* 95 (1994) 269.
- [12] A.E. Childress, M. Elimelech, *Abstr. Pap. Am. Chem. Soc.* 212 (1996) 9-ENVR.
- [13] S.K. Hong, M. Elimelech, *J. Membr. Sci.* 132 (1997) 159.
- [14] X.H. Zhu, M. Elimelech, *Environ. Sci. Technol.* 31 (1997) 3654.
- [15] M. Nystrom, H.H. Zhu, *J. Membr. Sci.* 131 (1997) 195.
- [16] M. Pontie, X. Chasseray, D. Lemordant, J.M. Laine, *J. Membr. Sci.* 129 (1997) 125.
- [17] M. Pontie, L. Durandbourlier, D. Lemordant, J.M. Laine, *J. Chim. Phys. Phys.-Chim. Biol.* 94 (1997) 1741.
- [18] A.E. Yaroshchuk, *Colloids Surf. A: Physicochem. Eng. Aspects* 140 (1998) 169.
- [19] A.E. Yaroshchuk, *Adv. Colloid Interface Sci.* 60 (1995) 1.
- [20] S.X. Li, D.B. Pengra, P.Z. Wong, *Phys. Rev. E* 51 (1995) 5748.
- [21] S.R. Caplan, A. Essig, *Bioenergetics and Linear Nonequilibrium Thermodynamics: the Steady State*, Harvard University Press, Cambridge, MA, 1983.
- [22] V. Compañ, T.S. Sørensen, A. Andrio, L. Lopez, J. Deabajo, *J. Membr. Sci.* 123 (1997) 293.
- [23] V. Compañ, M.L. Lopez, T.S. Sørensen, J. Garrido, *J. Phys. Chem.* 98 (1994) 9013.
- [24] V. Compañ, T.S. Sørensen, S.R. Rivera, *J. Phys. Chem.* 99 (1995) 12553.
- [25] A.E. Yaroshchuk, A.L. Makovetskiy, Yu. P. Boiko, E.W. Galinker, *J. Membr. Sci.* 172 (1–2) (2000) 203.
- [26] S. Koter, personal communication, 1999.
- [27] T. Okada, S.K. Ratkje, H. Hanche-Olsen, *J. Membr. Sci.* 66 (1992) 179.
- [28] E.K. Zholkovskij, *J. Colloid Interface Sci.* 169 (1995) 267.
- [29] E.K. Zholkovskij, in: T.S. Sørensen (Ed.), *Surface Chemistry and Electrochemistry of Membranes*, Marcel Dekker, New York, 1999.
- [30] O.V. Bobreshova, P.I. Kulintsov, E.M. Balavadze, *J. Membr. Sci.* 101 (1995) 1.